A bifunctional kinase-phosphatase in bacterial chemotaxis

Steven L. Porter, Mark A. J. Roberts, Cerys S. Manning, and Judith P. Armitage[1]

Oxford Centre for Integrative Systems Biology and Department of Biochemistry, University of Oxford, South Parks Road, Oxford OX1 3QU, United Kingdom

Edited by Thomas J. Silhavy, Princeton University, Princeton, NJ, and approved September 25, 2008 (received for review August 13, 2008)

Phosphorylation-based signaling pathways employ dephosphorylation mechanisms for signal termination. Histidine to aspartate phosphosignaling in the two-component system that controls bacterial chemotaxis has been studied extensively. *Rhodobacter sphaeroides* has a complex chemosensory pathway with multiple homologues of the *Escherichia coli* chemosensory proteins, although it lacks homologues of known signal-terminating CheY-P phosphatases, such as CheZ, CheC, FliY or CheX. Here, we demonstrate that an unusual CheA homologue, $CheA_3$, is not only a phosphodonor for the principal CheY protein, $CheY_6$, but is also a specific phosphatase for $CheY_6$-P. This phosphatase activity accelerates $CheY_6$-P dephosphorylation to a rate that is comparable with the measured stimulus response time of approximately 1 s. $CheA_3$ possesses only two of the five domains found in classical CheAs, the Hpt (P1) and regulatory (P5) domains, which are joined by a 794-amino acid sequence that is required for phosphatase activity. The P1 domain of $CheA_3$ is phosphorylated by $CheA_4$, and it subsequently acts as a phosphodonor for the response regulators. A $CheA_3$ mutant protein without the 794-amino acid region lacked phosphatase activity, retained phosphotransfer function, but did not support chemotaxis, suggesting that the phosphatase activity may be required for chemotaxis. Using a nested deletion approach, we showed that a 200-amino acid segment of $CheA_3$ is required for phosphatase activity. The phosphatase activity of previously identified nonhybrid histidine protein kinases depends on the dimerization and histidine phosphorylation (DHp) domains. However, $CheA_3$ lacks a DHp domain, suggesting that its phosphatase mechanism is different from that of other histidine protein kinases.

response regulator | signal termination | two-component | *Rhodobacter sphaeroides* | histidine protein kinase

Dephosphorylation is required for signal termination in phosphorylation-based signaling pathways. The most common phosphorylation-based signaling pathways in bacteria are two-component signal transduction systems, which can detect and mediate responses to a wide range of different environmental stimuli, with some bacteria having over 100 distinct systems (1, 2). These systems comprise sensor histidine protein kinases (HPKs) and response regulators (RRs). HPKs detect sensory stimuli; these regulate the rate at which the HPK autophosphorylates a conserved histidine residue. Subsequently, the phosphoryl group is transferred from the histidine residue of the HPK onto an aspartate residue in the receiver domain of the RR. Phosphorylation of the RR causes a conformational change, allowing it to mediate an output appropriate to the original stimulus, often a change in transcription (3). The phosphosignal is terminated by the hydrolysis of the aspartyl-phosphate residue of the RR.

Receiver domains have intrinsic autodephosphorylation activity, although in many systems a dedicated specific aspartyl-phosphate phosphatase is used to accelerate this process. Such phosphatases can be found in separate protein molecules, for example, RapA and CheZ dephosphorylate Spo0F-P and CheY-P, respectively (4, 5); alternatively, phosphatases can be integral parts of the HPKs. Hybrid HPKs, which are components of multistep phosphorelays, contain one or more receiver domains and all show phosphatase activity because of the autodephosphorylation activity of their receiver domains (6). Many nonhybrid HPKs also show phosphatase activity, for example, NtrB and EnvZ dephosphorylate their RRs, NtrC-P and OmpR-P, respectively (7, 8). The dimerization and histidine phosphorylation (DHp) domain of these HPKs has been implicated in the phosphatase reaction (8, 9). In this study, we report the discovery of an aspartyl-phosphatase activity within the chemotaxis protein, $CheA_3$, of *Rhodobacter sphaeroides*. Interestingly, unlike all previously identified nonhybrid HPKs with phosphatase activity, $CheA_3$ lacks a DHp domain and is not homologous to known phosphatases, suggesting that the $CheA_3$ phosphatase activity is novel.

The two-component system controlling chemotaxis allows bacteria to move toward environments that are better for growth [reviewed in (10–12)]. Chemoreceptors modulate the autophosphorylation rate of CheA in response to chemotactic stimuli. In *E. coli*, unliganded receptors activate CheA, whereas attractant-occupied receptors inhibit CheA autophosphorylation. The phosphoryl group is transferred from CheA-P to specific aspartate residues on its cognate RRs, CheY and CheB. CheY-P binding to the FliM component of the flagellar motor brings about a change in flagellar rotation and therefore swimming direction, while CheB-P demethylates the chemoreceptors, mediating adaptation. Hydrolysis of the phosphoryl-aspartate residues in CheY-P and CheB-P allows signal termination. *E. coli* CheY-P autodephosphorylates with a half-time of approximately 14 s (13); however, the phosphatase CheZ can increase this rate by a factor of approximately 100 (14). Many bacteria lack CheZ homologues and some of these instead use CheY-P phosphatases belonging to the CheC/FliY/CheX family of proteins (15–17). Other bacteria, including *Sinorhizobium meliloti* and *R. sphaeroides*, do not have homologues of any of these CheY-P phosphatases but do have multiple CheYs. *S. meliloti* has two CheYs, one that can bind the motor, CheY2, and one that cannot bind the motor, CheY1. CheY1 mediates dephosphorylation of CheY2-P by functioning as a phosphate sink (18). Like *S. meliloti* CheY2 but unlike *S. meliloti* CheY1, all of the *R. sphaeroides* CheYs are capable of binding to FliM, suggesting that a phosphate sink may not be used for signal termination in the *R. sphaeroides* chemotaxis pathway (19).

R. sphaeroides has two sets of flagellar genes and three chemotaxis operons (20). The fla1 set encodes a single unidirectional flagellum that is controlled by the chemotaxis proteins encoded by *che*Op_2 and *che*Op_3 (21), whereas the fla2 set encodes polar flagella that are controlled by *che*Op_1 (22, 23). *R.*

Author contributions: S.L.P. designed research; S.L.P., M.A.J.R., and C.S.M. performed research; S.L.P. contributed new reagents/analytic tools; S.L.P., M.A.J.R., C.S.M., and J.P.A. analyzed data; and S.L.P., M.A.J.R., and J.P.A. wrote the paper.

The authors declare no conflict of interest.

This article is a PNAS Direct Submission.

[1]To whom correspondence should be addressed: E-mail: armitage@bioch.ox.ac.uk.

This article contains supporting information online at www.pnas.org/cgi/content/full/0808010105/DCSupplemental.

sphaeroides has four CheA homologues. Phosphosignaling from $CheA_2$, $CheA_3$, and $CheA_4$ is essential for fla1 driven chemotaxis (24). $CheA_2$ localizes with the transmembrane chemoreceptors to the cell poles, whereas $CheA_3$ and $CheA_4$ localize to a cytoplasmic chemotaxis cluster along with the cytoplasmic chemoreceptors (25). $CheA_1$, $CheA_2$, and *E. coli* CheA function as homodimers. Each protomer contains five domains (P1–P5) with the P3 domain mediating dimerization. In *E. coli*, the P5 domain has been shown to bind CheW and the chemoreceptors and to couple the rate of CheA autophosphorylation to receptor control. During the autophosphorylation reaction, the kinase domain (P4) phosphorylates the histidine residue within the Hpt (P1) domain using ATP as the phosphodonor. The phosphorylated P1 domain donates phosphoryl groups to aspartate residues on CheY and CheB. The P2 domain binds CheY and CheB and therefore increases their local concentrations, accelerating the phosphotransfer reaction mediated by the P1 domain. $CheA_3$ and $CheA_4$ from *R. sphaeroides* are atypical CheAs in that they each lack some of the domains found in *E. coli* CheA. $CheA_4$ is a homodimeric protein containing only the P3, P4, and P5 domains whereas $CheA_3$ has only the P1 and P5 domains, separated by a 794-amino acid sequence containing no identifiable domains. $CheA_3$ and $CheA_4$ both localize to the cytoplasmic chemotaxis cluster (25). Neither $CheA_3$ nor $CheA_4$ are capable of autophosphorylation; however, $CheA_4$ can phosphorylate the P1 domain of $CheA_3$ on residue H51. Subsequently $CheA_3$-P acts as a phosphodonor for a specific subset of the chemotaxis RRs (24).

R. sphaeroides has eight chemotaxis RRs, six CheYs and two CheBs. While both CheBs are required for normal chemotaxis, only $CheY_6$ plus either $CheY_3$ or $CheY_4$ are needed for control of the fla1 flagellum (21, 26). The CheAs all show different patterns of phosphotransfer to the RRs: $CheA_1$-P phosphorylates $CheY_1$, $CheY_2$, $CheY_3$, and $CheY_5$; $CheA_2$-P phosphorylates all eight chemotaxis RRs; and $CheA_3$-P phosphorylates $CheY_1$, $CheY_6$, and $CheB_2$ (24, 27). Here, we demonstrate an additional activity for $CheA_3$, the ability to specifically catalyze the hydrolysis of the aspartyl-phosphate residue in $CheY_6$-P.

Results

P1 Domain of $CheA_3$ Is a Specific Phosphodonor for $CheY_1$, $CheY_6$, and $CheB_2$. $CheA_3$-P is a phosphodonor for only $CheY_1$, $CheY_6$, and $CheB_2$ (24). To determine whether this specificity depends solely on the interactions between the RRs and the P1 domain of $CheA_3$, phosphotransfer experiments were performed comparing the specificity of the isolated P1 domain of $CheA_3$ ($CheA_3$P1) with that of full-length $CheA_3$. Transfer of phosphoryl groups to the eight chemotaxis RRs was measured under multiple turnover conditions in the presence of $CheA_4$ and ATP, allowing either the $CheA_3$ or $CheA_3$P1 phosphorylation to continue throughout the course of the reactions. The progress of these phosphotransfer reactions after 30 s is shown in Fig. 1. Phosphotransfer occurred in reactions where a decrease in $CheA_3$-P or $CheA_3$P1-P levels was accompanied by an increase in CheY/B-P levels. $CheA_3$-P and $CheA_3$P1-P phosphorylated the same RRs ($CheY_1$, $CheY_6$, and $CheB_2$) indicating that it is the interaction between the RRs and the P1 domain of $CheA_3$-P that determines the phosphotransfer specificity of $CheA_3$-P. Interestingly, despite using equimolar concentrations of phosphodonor, $CheY_6$-P levels were greater when $CheA_3$P1-P was used as the phosphodonor rather than $CheA_3$-P. One possible explanation for this is that full-length $CheA_3$ is both a phosphodonor and a phosphatase for $CheY_6$-P. The isolated $CheA_3$P1 domain would lack this phosphatase activity, retaining only phosphodonor function and allowing more $CheY_6$-P to accumulate.

$CheA_3$ Is a Specific Phosphatase for $CheY_6$-P. The ability of $CheA_3$ to act as a chemotaxis RR phosphatase was measured in vitro by using a RR dephosphorylation assay that quantified the loss of ^{32}P-labeled phosphoryl groups from RR-P as a function of time. Parallel time course experiments were performed where a phosphodonor (either $CheA_3$P1-^{32}P or $CheA_2$-^{32}P) was mixed with a vast excess of RR (400 μM) in the presence and absence

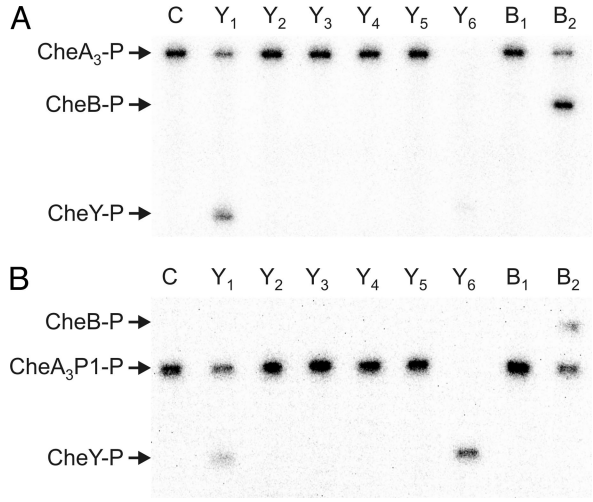

Fig. 1. Phosphorimages of SDS/PAGE gels showing phosphotransfer from (*A*) $CheA_3$ and (*B*) $CheA_3$P1 (the isolated P1 domain of $CheA_3$) to the *R. sphaeroides* chemotaxis response regulators. $CheA_3$ (4 μM) and $CheA_4$ (10 μM) were preincubated together with 0.5 mM [γ-^{32}P] ATP for 30 min. RRs (5 μM) were then added. Ten-microliter reaction samples were removed after 30 s and quenched in 10 μl of 3× SDS/EDTA loading dye. The samples were analyzed by SDS/PAGE and detected by phosphorimaging. Lane C shows a control reaction in which an equal volume of buffer was added instead of the RRs. The remaining lanes are labeled according to which RR was used; for example, $CheY_1$ was used in the lane labeled Y_1. Phosphotransfer is indicated by the appearance of phosphorylated RR and a reduction in the amount of (*A*) $CheA_3$-P or (*B*) $CheA_3$P1-P.

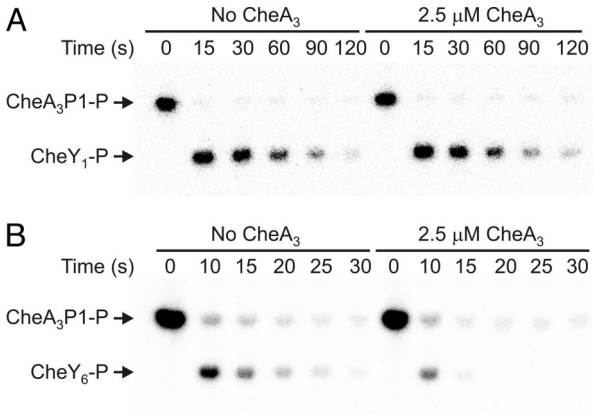

Fig. 2. Phosphorimages of SDS/PAGE gels showing the response regulator dephosphorylation time courses. (*A*) 400 μM $CheY_1$ was added to 2 μM $CheA_3$P1-P in the absence (left half of gel) and presence of 2.5 μM $CheA_3$ (right half of gel). (*B*) 400 μM $CheY_6$ was added to 30 μM $CheA_3$P1-P in the absence (left half of gel) and presence of 2.5 μM $CheA_3$ (right half of gel). 10-μl reaction samples were taken at the time points indicated and quenched in 20 μl of 1.5× SDS/EDTA loading dye. The quenched samples were analyzed by SDS/PAGE and detected by phosphorimaging. ATP was not present in any of the reactions, so after the phosphotransfer reactions, which were completed before the first-time point, the only reaction occurring was RR-P dephosphorylation. As has been observed for *E. coli* CheA, a small fraction of $CheA_3$P1-P ($<$ 4%) failed to transfer phosphoryl groups to the RRs (42). Phosphatase activity is indicated by a reduction in CheY-P levels in the presence of 2.5 μM $CheA_3$ when compared with those in the absence of $CheA_3$ (seen in *B* but not in *A*).

Table 1. The effect of $CheA_3$ on the dephosphorylation rates of the *R. sphaeroides* CheY/Bs

Protein	Dephosphorylation half-time, s*	
	0 μM $CheA_3$†	2.5 μM $CheA_3$‡
$CheY_1$-P	27 ± 1	27 ± 1
$CheY_2$-P	63 ± 3	67 ± 4
$CheY_3$-P	36 ± 3	40 ± 4
$CheY_4$-P	38 ± 3	39 ± 2
$CheY_5$-P	27 ± 1	30 ± 1
$CheY_6$-P	4.1 ± 0.3	1.4 ± 0.1
$CheB_1$-P	4000 ± 200	4100 ± 100
$CheB_2$-P	52 ± 4	52 ± 7

*, Mean ± standard error (values rounded to two significant figures). Each experiment was performed six times.

†While most of these values are in good agreement with our previous estimates of dephosphorylation rate, some of these values differ considerably from our earlier estimates (27). The values in this table were derived from a direct assay of RR-P dephosphorylation and are more accurate. The previous estimates were based on an indirect assay that examined the steady state concentration of phosphorylated response regulator in a reaction mixture containing $CheA_2$ and ATP, and consequently were very sensitive to small errors in measuring the $CheA_2$ autophosphorylation rate and the steady state [CheY/B-P] and [$CheA_2$-P].

‡The molar ratio of RR to $CheA_3$ was 160:1.

of the putative phosphatase, $CheA_3$ (Fig. 2 and Table 1). After phosphotransfer, no rephosphorylation of the phosphodonor could occur because ATP was not present. Under these conditions, phosphotransfer from phosphodonor to the RR occurred rapidly and was complete before the first time point. Therefore, the only reaction occurring after the first time point was the dephosphorylation of the phosphorylated RR that had been generated by the phosphotransfer reaction. By monitoring the subsequent decrease in RR-P levels over time it was possible to measure the dephosphorylation rate constant by fitting the time course data to a first order exponential decay model (Table 1). No significant change in $CheY_{1-5}$-P or $CheB_{1\&2}$-P dephosphorylation rate constants was observed in the presence of $CheA_3$ (Fig. 2*A* and Table 1), indicating that $CheA_3$ is not a phosphatase for these RRs. In contrast, $CheY_6$-P levels fell faster in the presence of $CheA_3$ than in the absence of $CheA_3$ indicating that $CheA_3$ is a phosphatase for $CheY_6$-P (Fig. 2*B* and Table 1). Under these reaction conditions, where the concentration of $CheA_3$ used was 2.5 μM and the $CheY_6$ concentration was 400 μM, giving a molar ratio of $CheY_6$ to $CheA_3$ of 160:1, $CheA_3$ increased the dephosphorylation rate of $CheY_6$-P by a factor of three. No $CheA_3$-P was detected at any point in the assay (Fig. 2*B*), suggesting that the phosphatase mechanism does not involve reversed phosphotransfer to $CheA_3$. The effect of varying [$CheA_3$] on the rate of $CheY_6$-P dephosphorylation is shown in the supporting information (SI) *Text*, and Fig. S1. In summary, $CheA_3$ is an aspartyl-phosphate phosphatase that is specific for $CheY_6$-P.

Requirements for $CheA_3$ Phosphatase Activity. To determine whether the phosphorylation site (H51) of $CheA_3$ has any involvement in phosphatase activity, as has been seen for other HPKs with intrinsic phosphatase activity, the phosphatase activity of $CheA_3$(H51Q) was measured. The phosphatase activities of $CheA_3$ and $CheA_3$(H51Q) were indistinguishable, indicating that the phosphorylation site (H51) of $CheA_3$ has no role in phosphatase activity (Fig. 3).

The $CheA_3$(Δ155–948) mutant protein retains only the P1 and P5 domains and lacks the intervening 794-amino acid region. Like the isolated $CheA_3$P1 domain, the $CheA_3$(Δ155–948) mutant protein was phosphorylatable by $CheA_4$ and functioned as a phosphodonor for the cognate RRs of $CheA_3$ (data not shown). This mutant protein did not, however, show any $CheY_6$-P phosphatase activity (Fig. 3), indicating that either the deleted 794-amino acid region is required for phosphatase activity or that this large deletion causes misfolding of the remainder of the protein such that phosphatase activity but not phosphodonor ability was abolished. The 794-amino acid region of $CheA_3$ was then arbitrarily subdivided into four sub-regions (Fig. 3). Mutant $CheA_3$ proteins with various nested deletions of these regions were purified and assayed for $CheY_6$-P phosphatase activity. The P5 domain and sub-region 4 were not required for phosphatase activity. Sub-region 3 (residues 549–749) was essential for phosphatase activity, while deletion of sub-region 2 or sub-regions 1 and 2 together caused a partial reduction in phosphatase activity (Fig. 3). The sequence in sub-regions 1 and 2 may therefore either be required for correct folding of the phosphatase activity or may have a regulatory effect on the phosphatase activity. Sub-region 3 (residues 549–749) was the only segment of $CheA_3$ that was been shown to be essential for phosphatase activity and is therefore presumed to contain the phosphatase activity. Within sub-region 3, there is a partial match to the consensus sequence of CheC-type phosphatases (*SI Text*). However, changing the predicted catalytic residues (E585 and N588) did not alter phosphatase activity (Fig. 3), indicating that $CheA_3$ is not a homologue of CheC.

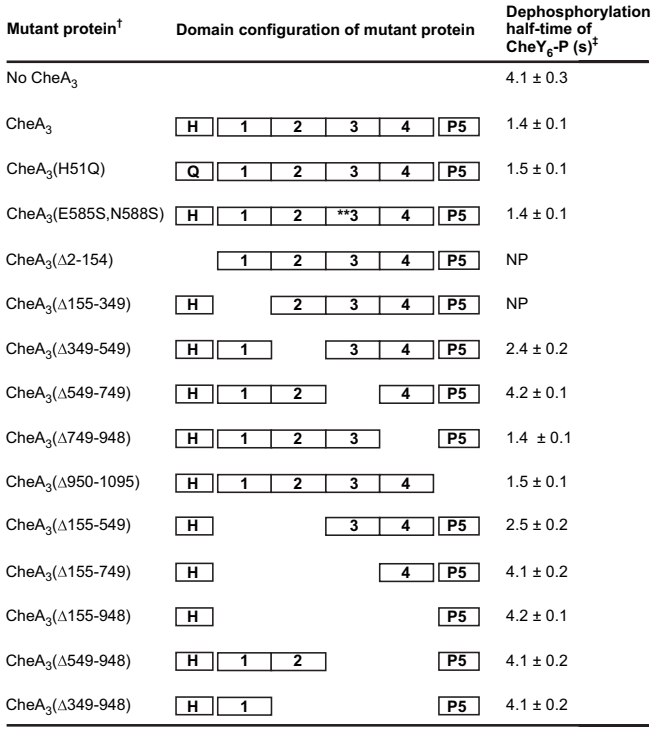

Fig. 3. The effect of $CheA_3$ mutant proteins on the dephosphorylation rate of $CheY_6$-P. †Two and one-half μM of each $CheA_3$ mutant protein was used in the phosphatase assays. The molar ratio of $CheY_6$ to $CheA_3$ mutant protein was 160:1. ‡Each experiment was performed six times and mean values ± standard error are shown (values are rounded to two significant figures). NP, could not be overexpressed and purified.

$CheA_3$(Δ155–948) Localizes Correctly but Does Not Support Chemotaxis. $CheA_3$ has previously been shown to localize to the cytoplasmic chemotaxis cluster along with $CheW_4$, $CheA_4$ and the putative cytoplasmic chemoreceptors (25). Localization of $CheA_3$ to this cluster may be required for it to function in the chemotaxis signal

MICROBIOLOGY

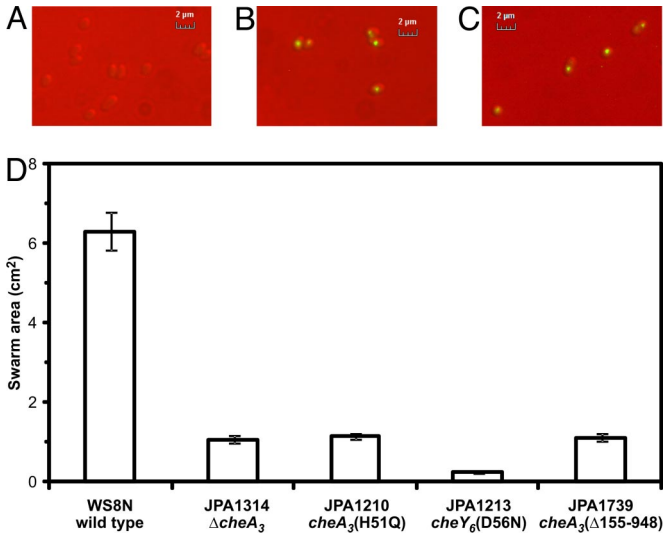

Fig. 4. The 794-amino acid region between the P1 and P5 domains of $CheA_3$ is not required for $CheA_3$ localization but is required for chemotaxis. (*A*) YFP fluorescence image of wild-type cells (strain WS8N). (*B*) YFP fluorescence image of JPA1425 (*yfp-cheA*$_3$). (*C*) YFP fluorescence image of JPA1741 [*yfp-cheA*$_3$(Δ155–948)]. (*D*) Swarm plate chemotaxis assay comparing the chemotactic ability of JPA1739 [*cheA*$_3$(Δ155–948)] with wild-type (WS8N), nonchemotactic (JPA1314 and JPA1210) and nonmotile (JPA1213) strains. The swarm plates contained 100 μM propionate and were incubated for 48 h under aerobic conditions. Error bars show the standard error of the mean obtained from nine independent experiments.

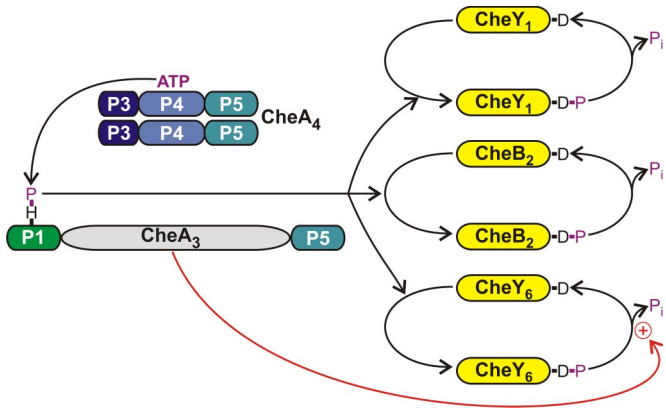

Fig. 5. The phosphorylation reactions involving $CheA_3$. The domain structures of $CheA_3$ and $CheA_4$ are shown. The P1 domain of $CheA_3$ is phosphorylated by a $CheA_4$ dimer. $CheA_3$-P then acts as a phosphodonor for either $CheY_1$, $CheY_6$, or $CheB_2$. These RRs all autodephosphorylate. However, $CheA_3$ acts as a phosphatase on $CheY_6$-P (red arrow) and can accelerate the rate of dephosphorylation by at least a factor of 3 over the rate of autodephosphorylation.

transduction system; therefore, the localization of $CheA_3$(Δ155–948) was examined by replacing the wild-type *cheA*$_3$ gene in the *R. sphaeroides* genome with *yfp-cheA*$_3$(Δ155–948), generating strain JPA1741. YFP-$CheA_3$(Δ155–948) localized to the cytoplasmic chemotaxis cluster in a pattern indistinguishable from that of YFP-$CheA_3$ (Fig. 4 *A–C*), indicating that the localization determinants for $CheA_3$ were still present and correctly folded in $CheA_3$(Δ155–948). Western blotting using an antibody that recognizes YFP showed that expression levels of YFP-$CheA_3$ and YFP-$CheA_3$(Δ155–948) were similar (data not shown).

$CheA_3$(Δ155–948) retains all of the known activities of full-length $CheA_3$ except for the phosphatase activity, that is, it can be phosphorylated by $CheA_4$, is a specific phosphodonor for the cognate RRs of full-length $CheA_3$, is expressed at wild-type levels in *R. sphaeroides*, and localizes to the cytoplasmic chemotaxis cluster. To assess the importance of the $CheY_6$-P phosphatase activity *in vivo*, the *cheA*$_3$ gene in the *R. sphaeroides* genome was replaced with *cheA*$_3$(Δ155–948). As expected, and unlike the Δ*cheA*$_3$ strain, the *cheA*$_3$(Δ155–948) strain was capable of responding to step changes in chemoeffector concentration (1 mM to 0 mM sodium propionate) in tethered cell assays (data not shown), suggesting that $CheA_3$(Δ155–948) is capable of transducing signals *in vivo*. However, the *cheA*$_3$(Δ155–948) strain was nonchemotactic in swarm plate assays (Fig. 4*D*), suggesting that although cells lacking the phosphatase activity of $CheA_3$ are capable of responding to changes in chemoeffector levels, they do so in a time frame that is too slow to allow migration up a chemoeffector gradient. The lack of chemotaxis exhibited by the *cheA*$_3$(Δ155–948) strain suggests that the phosphatase activity of $CheA_3$ may be required for chemotaxis.

Discussion

In this study, we have shown that $CheA_3$ is a aspartyl-phosphate phosphatase that is specific for $CheY_6$-P. $CheA_3$ localizes with its partner protein $CheA_4$ to the cytoplasmic chemotaxis cluster (25), where $CheA_4$ phosphorylates $CheA_3$ (24). $CheA_3$-P is a phosphodonor for $CheY_1$, $CheY_6$, and $CheB_2$ (Fig. 5). Chemotactic stimuli, possibly reflecting the metabolic state of the cell, are presumed to control the rate at which $CheA_4$ phosphorylates $CheA_3$ (12). Both $CheA_3$ and $CheA_4$ contain a P5 (regulatory) domain, and the detection of phosphatase activity within $CheA_3$ raises the intriguing possibility that the phosphatase activity of $CheA_3$ and the kinase activity of $CheA_4$ could be reciprocally regulated by chemotactic stimuli. These results may also explain why the activities of $CheA_3$ and $CheA_4$ are encoded within separate proteins rather than within a single polypeptide chain. The chemotactic response of *R. sphaeroides* has been shown to depend on growth conditions (12). Variation of the expression levels of $CheA_3$ relative to that of $CheA_4$ would alter the phosphatase to kinase ratio and could allow tuning of the $CheY_6$-P output of the signaling pathway according to growth conditions. Consistent with this hypothesis, an internal promoter has recently been discovered within *che*Op$_3$ that could allow $CheA_3$ and $CheA_4$ expression levels to be independently regulated (M. Gould, M.A.J.R., and J.P.A., unpublished work).

$CheA_3$ Phosphatase Activity. Outside of chemotaxis, many nonhybrid histidine protein kinases have built in aspartyl-phosphatase activity (28, 29); some of the most extensively studied examples are HPKs, NtrB, EnvZ, and PhoR. The phosphatase activity of these proteins has been shown to depend on their dimerization and histidine phosphorylation (DHp) domains (8, 9, 29). Interestingly, the DHp domain is not present in $CheA_3$, suggesting that the phosphatase activity of $CheA_3$ differs substantially from those found in previously characterized HPKs.

The ability of the $CheA_3$ phosphorylation site mutant protein, $CheA_3$(H51Q) to act as a phosphatase indicates that the $CheY_6$-P dephosphorylation mechanism used by $CheA_3$ does not require reversed phosphotransfer from $CheY_6$-P to $CheA_3$. Deletion of the 794-amino acid region between the P1 and P5 domains of $CheA_3$ abolished the $CheY_6$-P phosphatase activity (Fig. 3) but not the ability of the protein to be phosphorylated by $CheA_4$ and subsequently act as a phosphodonor for its RRs. Nested deletion analysis showed that residues 549–749 (subregion 3) are essential for phosphatase activity, and because no other region of $CheA_3$ was shown to be essential for phosphatase activity, the phosphatase activity presumably resides within this sequence. The entire 794-amino acid region contains no known conserved domains although homologues have been identified in *Roseovarius* sp. TM1035 (RefSeq accession:

ZP_01878577) and in a marine metagenomic sample obtained from a hypersaline lagoon in the Galapagos Islands (CAMERA accession: JCVI_PEP_1105096654245) (30), suggesting that a range of different bacteria may employ this phosphatase activity in their signal transduction pathways.

Relevance of the $CheA_3$ Phosphatase to Chemotactic Signaling. *E. coli* CheY-P autodephosphorylates with a half-time of approximately 14 s (13), and its phosphatase, CheZ, can accelerate this by a factor of 100 (14) to approximately 0.14 s. This dramatic stimulation of CheY-P dephosphorylation is required because the stimulus response time of *E. coli* is approximately 0.2 s (31) and signal termination needs to occur on a comparable time scale (32). When comparing the phosphatase activity of $CheA_3$ toward $CheY_6$-P with *E. coli* CheZ toward CheY-P, the phosphatase activity of $CheA_3$ appears modest giving a 3-fold versus a 100-fold stimulation, respectively. However, *R. sphaeroides* may not need such a potent phosphatase because $CheY_6$-P already has one of the fastest known dephosphorylation rates with an approximate half time of 4.1 s versus the 14-s half-time of *E. coli* CheY. In addition, the measured stimulus response time is slower for *R. sphaeroides* (~1 s) than *E. coli* (~0.2 s) (31, 33), possibly reflecting the requirement for transport and partial metabolism in *R. sphaeroides* chemotaxis (12). The enhancement of $CheY_6$-P dephosphorylation by $CheA_3$ reduces the half-time to 1.4 s, which is comparable with the stimulus response time of 1 s (33). The modest phosphatase activity of $CheA_3$ may therefore be critical for chemotaxis because this would bring the rate of $CheY_6$-P dephosphorylation within the physiological range required for efficient gradient sensing and chemotactic signaling. Consistent with this, *R. sphaeroides* strains without the 794-amino acid region of $CheA_3$ and therefore lacking phosphatase activity were nonchemotactic even though the remainder of the $CheA_3$ protein, $CheA_3$(Δ155–948), was expressed at wild-type levels and localized correctly to the cytoplasmic chemotaxis cluster (Fig. 4). These observations suggest that the phosphatase activity of $CheA_3$ is required to achieve a rapid rate of signal termination that is compatible with the chemotactic migration of cells in chemoeffector gradients.

Chemotaxis Phosphatase Localization. In this study, we have shown that $CheA_3$ is not only a phosphodonor for $CheY_6$, but is also a specific phosphatase for $CheY_6$-P. However, this colocalization of phosphotransfer and phosphatase functions is not restricted to $CheA_3$ and its close homologues. *Methanospirillum hungatei* JF-1 has a CheA-CheC fusion protein (RefSeq accession: YP_501607) that sequence analysis suggests would show CheY-P phosphatase activity (34). The CheY-P phosphatases, CheC from *B. subtilis* and CheX from *Treponema denticola*, both interact with CheA in two-hybrid assays, suggesting that the principle of colocalizing phosphotransfer and phosphatase activities is also used by these bacteria (35, 36). In *E. coli*, the chemotaxis phosphatase, CheZ, localizes to the polar chemoreceptor cluster via its interaction with $CheA_{short}$. This colocalization of the *E. coli* chemotaxis kinase and phosphatase at the cell poles prevents the formation of steep spatial gradients of CheY-P concentration that would otherwise form if the phosphatase was not localized at the cell poles and was instead distributed throughout the cytoplasm (37). This is important because steep gradients of CheY-P would expose each flagellar motor to different concentrations of CheY-P depending on their proximity to the chemoreceptor cluster and therefore motor switching would become a function of the distance between the motor and the chemoreceptor cluster (38, 39). In $CheA_3$, *R. sphaeroides* appears to have extended this network design principle by colocalizing phosphotransfer and phosphatase activities within the same protein molecule.

Methods

Plasmids and Strains. The plasmids and strains used are shown in Table S1. *E. coli* strains were grown in LB medium at 37°C. *R. sphaeroides* strains were grown in succinate medium at 30°C under aerobic conditions with shaking. Where required antibiotics were used at concentrations of 100 μg ml^{-1} for ampicillin and 25 μg ml^{-1} for kanamycin and nalidixic acid.

Molecular Genetic Techniques. All standard genetic techniques were performed as described (40). *Pfu* polymerase (Promega) was used for all PCRs. All primers were synthesized by Sigma-Genosys. DNA sequencing was performed by Geneservice (Department of Biochemistry, Oxford University).

Mutagenesis of *cheA*$_3$ in the *R. sphaeroides* Genome. Overlap extension PCR was used to generate constructs for (*i*) overexpressing mutant $CheA_3$ proteins and (*ii*) for replacing either *cheA*$_3$ in strain WS8N or *yfp-cheA*$_3$ in strain JPA1425 in the *R. sphaeroides* genome with mutant versions of *cheA*$_3$ (41).

Behavioral Analysis. The swarm plate and tethered cell responses to propionate of the *R. sphaeroides* strains were characterized as described previously (21). Swarm plates were used to assess motility by reference to known nonmotile, nonchemotactic, and chemotactic strains; nonmotile cells form smaller colonies on swarm plates than do motile but nonchemotactic cells that, in turn, form smaller colonies than chemotactic cells. Nine datasets were obtained.

Fluorescence Microscopy. DIC and fluorescence images of YFP fusion expressing *R. sphaeroides* strains were acquired as described previously (25). At least seven fields of view each containing at least 30 cells from independent cultures were analyzed for each strain.

Protein Purification. His-tagged and GST-tagged *R. sphaeroides* CheA, CheY, and CheB proteins were purified as described previously (24, 27). All $CheA_3$ derivatives were purified in the same way as wild-type $CheA_3$ (24). Protein purity and protein concentrations were measured as described (27). Purified proteins were stored at −20°C.

Phosphotransfer from $CheA_3$-P and $CheA_3$P1-P to the Response Regulators. Phosphotransfer assays were performed at 20°C in TGMNKD buffer (50 mM Tris·HCl, 10% (vol/vol) glycerol, 5 mM $MgCl_2$, 150 mM NaCl, 50 mM KCl, and 1 mM DTT, pH 8.0). Reaction mixtures contained 10 μM $CheA_4$ and either 4 μM $CheA_3$ or $CheA_3$P1. The reactions mixtures were incubated at 20°C for 1 h before addition of 0.5 mM [γ-^{32}P] ATP (specific activity 14.8 GBq mmol^{-1}; PerkinElmer). The ATP dependent phosphorylation of $CheA_3$/$CheA_3$P1 was allowed to proceed for 30 min and then the phosphotransfer reactions were initiated by the addition of 5 μM RR. Reaction aliquots of 10 μl of were taken after 30 s and quenched immediately in 5 μl of 3× SDS/PAGE loading dye (7.5% (wt/vol) SDS, 90 mM EDTA, 37.5 mM Tris·HCl, 37.5% glycerol, and 3% (vol/vol) β-mercaptoethanol, pH 6.8). Quenched samples were analyzed by using SDS/PAGE and phosphorimaging as described previously (27).

Preparation of $CheA_3$P1-^{32}P and $CheA_2$-^{32}P. Proteins were phosphorylated in reactions performed at 20°C in TGMNKD buffer. The final reaction volumes were 4.5 ml. For production of $CheA_3$P1-^{32}P, reaction mixtures contained 300 μM $CheA_3$P1 (His-tagged) and 20 μM $CheA_4$ (GST-tagged), while for production of $CheA_2$-^{32}P, reaction mixtures contained 60 μM $CheA_2$ (His-tagged). Reactions were initiated by addition of 0.5 mM [γ-^{32}P] ATP (specific activity 14.8 GBq mmol^{-1}). After a 1-h incubation, samples were purified by using Ni-NTA columns (Qiagen) as described previously for unphosphorylated His-tagged $CheA_2$ and $CheA_3$ (24, 27). This purification step removed the unincorporated ATP from the $CheA_2$-^{32}P and $CheA_3$P1-^{32}P preparations and also removed the GST-tagged $CheA_4$ protein from the $CheA_3$P1-P preparation as judged by Coomassie-stained SDS/PAGE gels of the eluted proteins. Purified proteins were stored at −20°C.

Dephosphorylation Assays. CheY/B-P dephosphorylation rates were measured by using a modification of the method previously described (42, 43). All assays were performed at 20°C in TGMNKD buffer. The final reaction volume was 150 μl. An excess of CheY/B (400 μM final concentration) was added to either $CheA_3$P1-^{32}P (for $CheY_1$, $CheY_6$, and $CheB_2$) or $CheA_2$-^{32}P (for $CheY_2$, $CheY_3$, $CheY_4$, $CheY_5$, and $CheB_1$); the phosphodonor used for each RR was chosen on the basis of fastest phosphotransfer rate. For all RRs except $CheY_6$, the concentration of phosphodonor used in these assays was 2 μM, although because of the rapid autodephosphorylation of $CheY_6$-P it was necessary to increase

MICROBIOLOGY

the concentration of $CheA_3P1$-^{32}P to 30 μM to obtain detectable levels of $CheY_6$-P throughout the 30-s time course. For assessing $CheA_3$ phosphatase activity, parallel reaction mixtures were set up with and without 2.5 μM $CheA_3$, allowing RR dephosphorylation rates to be compared in the presence and absence of $CheA_3$. After addition of the RR to the reaction mixture, 10-μl aliquots were removed at regular time intervals and quenched immediately in 20 μl of 1.5× SDS/PAGE loading dye. Six samples were taken for each time course. The duration of the time course was optimized according to the rate of dephosphorylation of each RR-P; for $CheY_6$ the time course covered 30 s, for $CheB_1$ the time course covered 3,600 s, and for all other RRs the time course covered 120 s. Quenched samples were analyzed by using SDS/PAGE and phosphorimaging as described previously (41). Owing to the vast molar excess of CheY/B used in these assays, the phosphotransfer reactions were completed within 10 s of mixing. Because ATP was not present in the reaction mixtures, no rephosphorylation of the phosphodonor occurred, so once the phosphotransfer reaction had completed (before the first time point), the only reaction occurring was CheY/B-P dephosphorylation. Consequently, by measuring the decrease in CheY/B-P levels over time, it was possible to directly calculate the dephosphorylation rate. All dephosphorylation reactions displayed kinetics that gave a good fit to single exponential decay ($R^2 > 0.998$) allowing the rate constants to be determined by using Microcal Origin software.

SI. Further information is available in *SI Text* and Fig. S2.

ACKNOWLEDGMENTS. This work was funded by the Biotechnology and Biological Sciences Research Council and Lincoln College, Oxford.

1. Stock AM, Robinson VL, Goudreau PN (2000) Two-component signal transduction. *Annu Rev Biochem* 69:183–215.
2. Ulrich LE, Zhulin IB (2007) MiST: A microbial signal transduction database. *Nucl Acids Res* 35:D386–D390.
3. Galperin MY (2006) Structural classification of bacterial response regulators: Diversity of output domains and domain combinations. *J Bacteriol* 188:4169–4182.
4. Perego M, *et al.* (1994) Multiple protein-aspartate phosphatases provide a mechanism for the integration of diverse signals in the control of development in *B. subtilis. Cell* 79:1047–1055.
5. Hess JF, Oosawa K, Kaplan N, Simon MI (1988) Phosphorylation of three proteins in the signalling pathway of bacterial chemotaxis. *Cell* 53:79–87.
6. West AH, Stock AM (2001) Histidine kinases and response regulator proteins in two-component signaling systems. *Trends Biochem Sci* 26:369–376.
7. Russo FD, Silhavy TJ (1991) EnvZ controls the concentration of phosphorylated OmpR to mediate osmoregulation of the porin genes. *J Mol Biol* 222:567–580.
8. Jiang P, Atkinson MR, Srisawat C, Sun Q, Ninfa AJ (2000) Functional dissection of the dimerization and enzymatic activities of *Escherichia coli* Nitrogen Regulator II and their regulation by the PII protein. *Biochemistry* 39:13433–13449.
9. Zhu Y, Qin L, Yoshida T, Inouye M (2000) Phosphatase activity of histidine kinase EnvZ without kinase catalytic domain. *Proc Natl Acad Sci USA* 97:7808–7813.
10. Wadhams GH, Armitage JP (2004) Making sense of it all: Bacterial chemotaxis. *Nat Rev Mol Cell Bio* 5:1024–1037.
11. Szurmant H, Ordal GW (2004) Diversity in chemotaxis mechanisms among the Bacteria and Archaea. *Microbiol Mol Biol Rev* 68:301–319.
12. Porter SL, Wadhams GH, Armitage JP (2008) Rhodobacter sphaeroides: Complexity in chemotactic signalling. *Trends Microbiol* 16:251–260.
13. Appleby JL, Bourret RB (1998) Proposed signal transduction role for conserved CheY residue Thr87, a member of the response regulator active-site quintet. *J Bacteriol* 180:3563–3569.
14. Silversmith RE, Levin MD, Schilling E, Bourret RB (2008) Kinetic characterization of catalysis by the chemotaxis phosphatase CheZ: Modulation of activity by the phosphorylated CheY substrate. *J Biol Chem* 283:756–765.
15. Szurmant H, Bunn MW, Cannistraro VJ, Ordal GW (2003) Bacillus subtilis hydrolyzes CheY-P at the location of its action: The flagellar switch. *J Biol Chem* 278:48611–48616.
16. Muff TJ, Foster RM, Liu PJY, Ordal GW (2007) CheX in the three-phosphatase system of bacterial chemotaxis. *J Bacteriol* 189:7007–7013.
17. Motaleb MA, *et al.* (2005) CheX is a phosphorylated CheY phosphatase essential for *Borrelia burgdorferi* chemotaxis. *J Bacteriol* 187:7963–7969.
18. Sourjik V, Schmitt R (1998) Phosphotransfer between CheA, CheY1, and CheY2 in the chemotaxis signal transduction chain of *Rhizobium meliloti. Biochemistry* 37:2327–2335.
19. Ferre A, de la Mora J, Ballado T, Camarena L, Dreyfus G (2004) Biochemical study of multiple CheY response regulators of the chemotactic pathway of *Rhodobacter sphaeroides. J Bacteriol* 186:5172–5177.
20. Mackenzie C, *et al.* (2001) The home stretch, a first analysis of the nearly completed genome of *Rhodobacter sphaeroides* 2.4.1. *Photosynth Res* 70:19–41.
21. Porter SL, Warren AV, Martin AC, Armitage JP (2002) The third chemotaxis locus of *Rhodobacter sphaeroides* is essential for chemotaxis. *Mol Microbiol* 46:1081–1094.
22. Poggio S, *et al.* (2007) A complete set of flagellar genes acquired by horizontal transfer coexists with the endogenous flagellar system in *Rhodobacter sphaeroides. J Bacteriol* 189:3208–3216.
23. del Campo AM, *et al.* (2007) Chemotactic control of the two flagellar systems of *Rhodobacter sphaeroides* is mediated by different sets of CheY and FliM proteins. *J Bacteriol* 189:8397–8401.
24. Porter SL, Armitage JP (2004) Chemotaxis in *Rhodobacter sphaeroides* requires an atypical histidine protein kinase. *J Biol Chem* 279:54573–54580.
25. Wadhams GH, Warren AV, Martin AC, Armitage JP (2003) Targeting of two signal transduction pathways to different regions of the bacterial cell. *Mol Microbiol* 50:763–770.
26. Porter SL, *et al.* (2006) The CheYs of *Rhodobacter sphaeroides. J Biol Chem* 281:32694–32704.
27. Porter SL, Armitage JP (2002) Phosphotransfer in *Rhodobacter sphaeroides* chemotaxis. *J Mol Biol* 324:35–45.
28. Raivio TL, Silhavy TJ (1997) Transduction of envelope stress in *Escherichia coli* by the Cpx two- component system. *J Bacteriol* 179:7724–7733.
29. Carmany DO, Hollingsworth K, McCleary WR (2003) Genetic and biochemical studies of phosphatase activity of PhoR. *J Bacteriol* 185:1112–1115.
30. Yooseph S, *et al.* (2007) The *Sorcerer II* global ocean sampling expedition: Expanding the universe of protein families. *PLoS Biol* 5:e16.
31. Segall JE, Manson MD, Berg HC (1982) Signal processing times in bacterial chemotaxis. *Nature* 296:855–857.
32. Berg HC, Purcell EM (1977) Physics of chemoreception. *Biophys J* 20:193–219.
33. Berry RM, Armitage JP (2000) Response kinetics of tethered *Rhodobacter sphaeroides* to changes in light intensity. *Biophys J* 78:1207–1215.
34. Wuichet K, Alexander RP, Zhulin IB (2007) Comparative genomic and protein sequence analyses of a complex system controlling bacterial chemotaxis. *Method Enzymol* 422:3–31.
35. Kirby JR, *et al.* (2001) CheC is related to the family of flagellar switch proteins and acts independently from CheD to control chemotaxis in *Bacillus subtilis. Mol Microbiol* 42:573–585.
36. Sim JH, Shi W, Lux R (2005) Protein–protein interactions in the chemotaxis signalling pathway of *Treponema denticola. Microbiology* 151:1801–1807.
37. Vaknin A, Berg HC (2004) Single-cell FRET imaging of phosphatase activity in the *Escherichia coli* chemotaxis system. *Proc Natl Acad Sci USA* 101:17072–17077.
38. Lipkow K, Andrews SS, Bray D (2005) Simulated diffusion of phosphorylated CheY through the cytoplasm of *Escherichia coli. J Bacteriol* 187:45–53.
39. Rao CV, Kirby JR, Arkin AP (2005) Phosphatase localization in bacterial chemotaxis: Divergent mechanisms, convergent principles. *Physical Biology* 2:148–158.
40. Sambrook J, Russell DW (2001) in *Molecular Cloning: A laboratory manual* (Cold Spring Harbor Laboratory Press, Woodbury, NY).
41. Porter SL, Wadhams GH, Armitage JP (2007) *In vivo* and *in vitro* analysis of the *Rhodobacter sphaeroides* chemotaxis signaling complexes. *Method Enzymol* 423:392–413.
42. Thomas SA, Brewster JA, Bourret RB (2008) Two variable active site residues modulate response regulator phosphoryl group stability. *Mol Microbiol* 69:453–465.
43. Silversmith RE, Appleby JL, Bourret RB (1997) Catalytic mechanism of phosphorylation and dephosphorylation of CheY: Kinetic characterization of imidazole phosphates as phosphodonors and the role of acid catalysis. *Biochemistry* 36:14965–14974.